

Short Communication

## Synthesis and Electrochemical Characteristics of $\text{Li}_3\text{V}_2(\text{PO}_4)_3/\text{C}$ as a Novel Li-ion Battery Cathode Material

Jingjing Zhu, Zhi Su\*

College of Chemistry and Chemical Engineering, Xinjiang Normal University, Urumqi, 830054  
Xinjiang, China

\*E-mail: [suzhixj@sina.com](mailto:suzhixj@sina.com)

Received: 7 November 2017 / Accepted: 5 January 2018 / Published: 5 February 2018

---

Herein, we describe the two-step synthesis of  $\text{Li}_3\text{V}_2(\text{PO}_4)_3/\text{C}$ , a novel Li-ion battery cathode material, and characterize it by X-ray diffraction, X-ray photoelectron spectroscopy, high-resolution transmission electron microscopy, and electrochemical methods. The obtained results reveal that the above composite has a monoclinic crystal structure and features a carbon-coated surface, consequently exhibiting increased conductivity. Constant current charge-discharge, cyclic voltammetry, and electrochemical impedance spectroscopy tests show that samples annealed at 800°C for 12h exhibit an increased discharge capacity of 130.8 mAh/g (which is close to the theoretical specific capacity of 133 mAh/g) and are characterized by high cycleability in the voltage range of 3.0–4.5 V at 0.1 C, e.g., a discharge capacity of 120.2 mAh/g is observed after 50 cycles, corresponding to a capacity retention of 91.9%.

---

**Keywords:** lithium-ion battery, cathode material,  $\text{Li}_3\text{V}_2(\text{PO}_4)_3/\text{C}$ , two-step synthesis.

### 1. INTRODUCTION

The global energy crisis necessitates the development of efficient and environmentally friendly power sources such as Li-ion batteries, which are widely used as advanced energy storage devices due to exhibiting high capacity, high rate capability, and long cycling lifetime[1-3]. Lithium ion battery is an advanced energy storage device for environmental protection. Notably, the performance and price of Li-ion batteries is significantly influenced by those of their cathode materials, making the design of such materials (e.g., LVP-based ones) a matter of great significance, particularly in view of the availability of phosphorus and vanadium resources in China.  $\text{Li}_3\text{V}_2(\text{PO}_4)_3$  has two crystal structures: monoclinic and rhombic crystal, the thermal stability of rhombic crystal structure  $\text{Li}_3\text{V}_2(\text{PO}_4)_3$  cathode material is very poor and can not be synthesized directly. monoclinic  $\text{Li}_3\text{V}_2(\text{PO}_4)_3$  has excellent

structural stability. Therefore, the  $\text{Li}_3\text{V}_2(\text{PO}_4)_3$  cathode material of monoclinic phase is mainly studied and introduced in this paper.  $\text{Li}_3\text{V}_2(\text{PO}_4)_3$ -based cathode materials can achieve a theoretical capacity of 133 mAh/g, with two Li ions being reversibly (de)intercalated in the potential range of 3.0–4.3V[4]. Nevertheless, the poor electronic conductivity ( $2.4 \times 10^{-7} \text{ S} \cdot \text{cm}^{-1}$ ) of pure  $\text{Li}_3\text{V}_2(\text{PO}_4)_3$  caused by the presence of isolated  $\text{VO}_6$  octahedral units hinders its practical applications[5]. Recently, the cycleability of  $\text{Li}_3\text{V}_2(\text{PO}_4)_3$  has been improved by doping and coating with carbon, whereas the corresponding ionic and electronic conductivities have been improved by modifying the preparation method.  $\text{Li}_3\text{V}_2(\text{PO}_4)_3$  material with excellent performance, this indicates that the material has attracted more and more attention in the related fields.  $\text{Li}_3\text{V}_2(\text{PO}_4)_3$  will also be the most likely substitute for commercial  $\text{LiFePO}_4$  electrode materials. Commonly,  $\text{Li}_3\text{V}_2(\text{PO}_4)_3$  is prepared using sol-gel[6-8], hydrothermal[9], and carbothermal reduction methods[10-11]. However, in this study, we describe an unprecedented two-step synthesis of  $\text{Li}_3\text{V}_2(\text{PO}_4)_3/\text{C}$ .

## 2. EXPERIMENTAL

All reagents were of analytical grade.  $\text{Li}_3\text{V}_2(\text{PO}_4)_3/\text{C}$  was prepared as follows. Aqueous  $\text{H}_2\text{O}_2$  (30 wt%) was slowly added to a solution of  $\text{V}_2\text{O}_5$  (5 mmol) in deionized water (30 mL), followed by the addition of  $\text{H}_3\text{PO}_4$  (10 mmol) and 30 wt% aqueous citric acid (20 mL). The obtained solids were dried at  $80^\circ\text{C}$  for 12h, dry glue evenly to the 10 mL crucible boat, ground, calcined in an atmosphere of Ar at  $900^\circ\text{C}$  for 6 h, and cooled to room temperature to obtain  $\text{VPO}_4/\text{C}$ .  $\text{CH}_3\text{COOLi} \cdot 2\text{H}_2\text{O}$  (15 mmol) and  $\text{H}_3\text{PO}_4$  (5 mmol) were dissolved in deionized water (20 mL), and the obtained mixture was ultrasonicated for 5 min to afford a gel that was dried at  $80^\circ\text{C}$  for 12h, cooled to room temperature, and ground to obtain  $\text{Li}_3\text{PO}_4$ . According to the mass ratio of the sample, deionized water and bead 1:1:4,  $\text{Li}_3\text{PO}_4$  (5 mmol) and  $\text{VPO}_4/\text{C}$  (10 mmol) were milled for 4h in a planetary ball mill, and the produced mixture was dried in a blast-drying box. The obtained powder was heated under Ar at  $350^\circ\text{C}$  for 4h in a tube furnace, which resulted in the evolution of  $\text{H}_2\text{O}$  and  $\text{CO}_2$ , and the residue was sintered at  $800^\circ\text{C}$  for 12h to obtain  $\text{Li}_3\text{V}_2(\text{PO}_4)_3/\text{C}$ . The crystal structure of the above composite was probed by X-ray diffraction (XRD; Bruker D2, Cu K radiation ( $= 1.5408 \text{ \AA}$ )), with spectra recorded for  $2\theta=10\text{--}60^\circ$ , whereas microstructural characterization was performed by transmission electron microscopy (TEM; JEN-2010FEE, Japan). The carbon content of the prepared samples was determined by elemental analysis (VarioEL 3, Elementar, Germany), and the oxidation states of constituent elements were determined by X-ray photoelectron spectroscopy (XPS; ESCALAB 250Xi-type analyzer, Thermo Fisher Scientific, USA, monochromatic Al K radiation).

To prepare  $\text{Li}_3\text{V}_2(\text{PO}_4)_3$  cathodes, a 1:1 (w/w) mixture of the active material and a solid conductive adhesive was treated with deionized water and homogenized, and the obtained slurry was coated onto aluminum foil that was then cut into 10-mm-diameter disks. The above disks were used to construct coin-type half-cells (LIR 2025) in an Ar-filled glove box. Li metal was used as an anode, and the electrolyte comprised a 1 M solution of  $\text{LiPF}_6$  in a 1:1:1 (v/v/v) mixture of ethylene methyl carbonate/ethylene carbonate/dimethyl carbonate. Charge-discharge behaviors and cycling performances were assessed at a current density of 0.1 C in a voltage range of 3.0–4.5V using a battery

tester (LAND CT2001A). Cyclic voltammetry (CV) measurements were performed in a voltage range of 3.0–4.5 V at a scan rate of  $0.1 \text{ mV s}^{-1}$ , and electrochemical impedance spectroscopy (EIS) tests were carried out at room temperature in a frequency range of 0.01 Hz to 0.1 MHz using an alternating-current voltage of 5 mV supplied by a CHI650D electrochemical work station.

### 3. RESULTS AND DISCUSSION

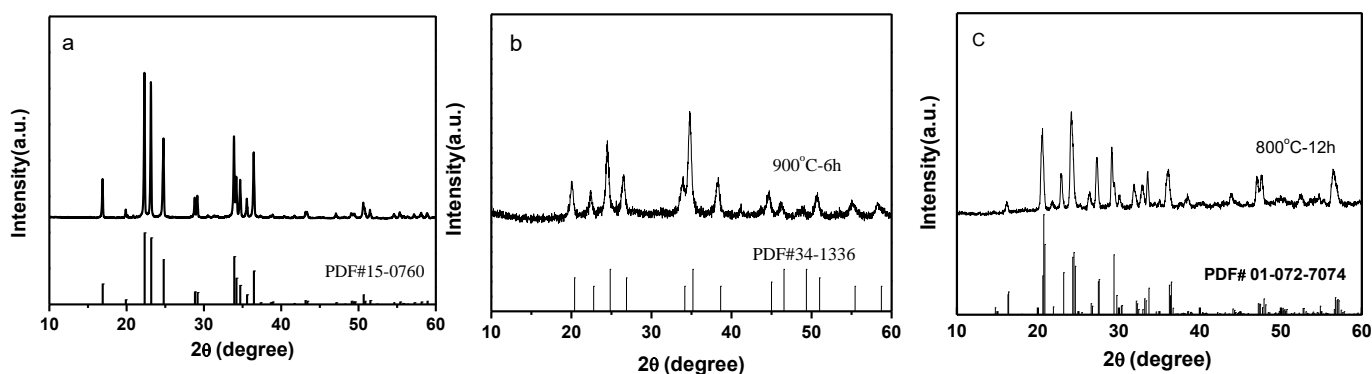


**Figure 1.** XRD patterns of the obtained  $\text{Li}_3\text{PO}_4$ (a),  $\text{VPO}_4/\text{C}$  calcined in a tube furnace under argon protection for  $900^\circ\text{C}-6\text{h}$  (b), and  $\text{Li}_3\text{V}_2(\text{PO}_4)_3/\text{C}$  materials calcined in a tube furnace under argon protection for  $850^\circ\text{C}-12\text{h}$  (c).

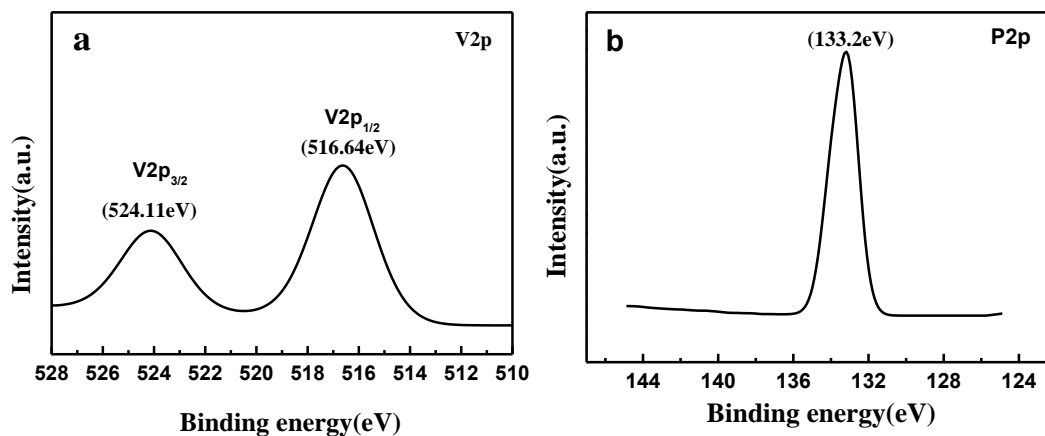


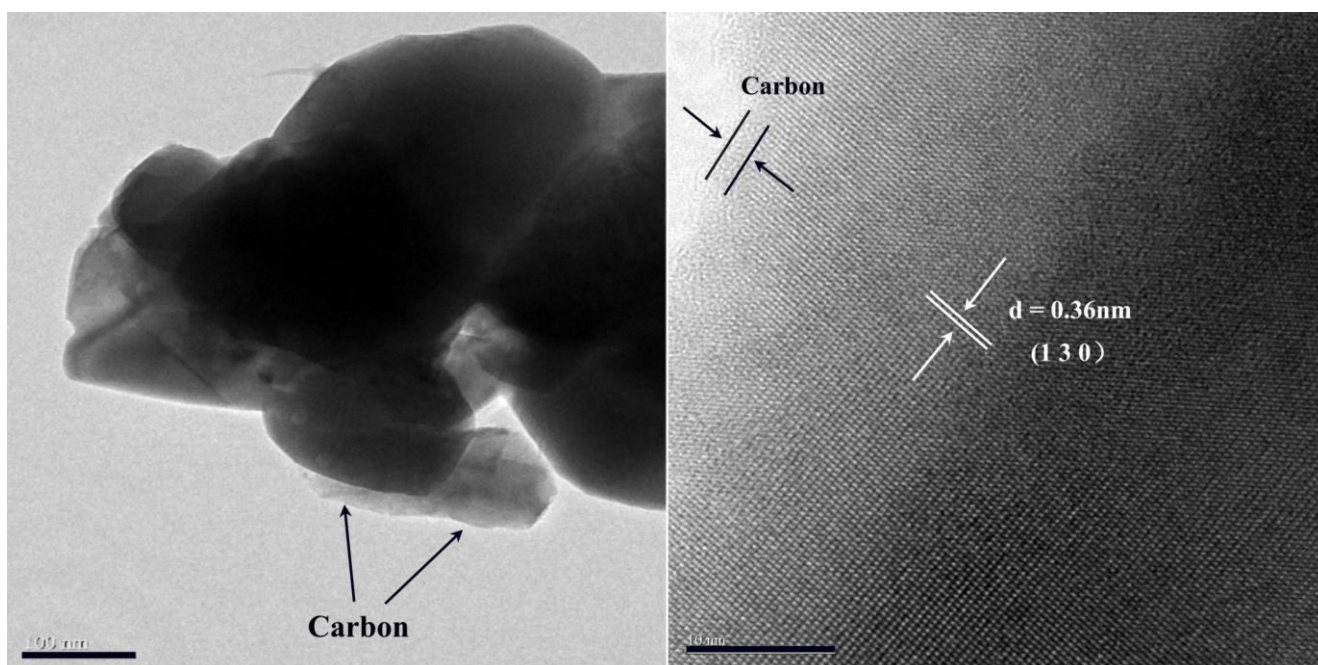
**Figure 2.** XPS core level of  $\text{Li}_3\text{V}_2(\text{PO}_4)_3/\text{C}$  materials about V2p (a) and P2p (b).

Figures 1(a–c) show the XRD patterns of as-prepared  $\text{Li}_3\text{PO}_4$ ,  $\text{VPO}_4/\text{C}$ , and  $\text{Li}_3\text{V}_2(\text{PO}_4)_3/\text{C}$ , respectively, with those of  $\text{Li}_3\text{PO}_4$  and  $\text{VPO}_4/\text{C}$  being in good agreement with the reference patterns of  $\text{Li}_3\text{PO}_4$  (PDF# 15-0760) and  $\text{VPO}_4$  (PDF# 34-1336), respectively. The XRD patterns of  $\text{Li}_3\text{V}_2(\text{PO}_4)_3/\text{C}$  and the monoclinic  $\text{Li}_3\text{V}_2(\text{PO}_4)_3$  standard (JCPDS No. 72-7074) shown in Fig.1c exhibit good agreement, with no impurity peaks observed. Since the lattice constants of  $\text{Li}_3\text{V}_2(\text{PO}_4)_3/\text{C}$  and the  $\text{Li}_3\text{V}_2(\text{PO}_4)_3$  standard were very close, we concluded that carbon had no obvious effect on the crystal structure of  $\text{Li}_3\text{V}_2(\text{PO}_4)_3$ , which was confirmed to exhibit a monoclinic crystal structure with a  $\text{P2}_1/\text{n}$  space group. In addition, the diffraction peaks of  $\text{Li}_3\text{V}_2(\text{PO}_4)_3$  were sharp, indicating that the obtained

composite was well-crystallized, with the absence of graphitized carbon peaks suggesting that the residual carbon in  $\text{Li}_3\text{V}_2(\text{PO}_4)_3/\text{C}$  was amorphous[12]. It is shown that the carbon in the outer layer of  $\text{Li}_3\text{V}_2(\text{PO}_4)_3$  exists in the form of uncertainty or less coated carbon and the form of carbon has no effect on the crystal structure of the material. Elemental analysis showed that the residual carbon content of  $\text{Li}_3\text{V}_2(\text{PO}_4)_3/\text{C}$  equaled 3.7%.

Figure 2 shows V2p and P2p XPS core level spectra of  $\text{Li}_3\text{V}_2(\text{PO}_4)_3/\text{C}$ , with Fig. 2b focusing on the local binding energy range of 510–528 eV and showing that peaks at 516.64 and 524.11 eV could be ascribed to  $\text{V}2\text{p}_{3/2}$  and  $\text{V}2\text{p}_{1/2}$  orbitals, respectively. Hence, it was concluded that V in  $\text{Li}_3\text{V}_2(\text{PO}_4)_3/\text{C}$  was present as  $\text{V}^{3+}$ [13]. Additionally, the corresponding P2p spectrum (Fig.2b) contained a single peak at 133.2eV. Thus, the obtained results were consistent with those of XRD analysis.

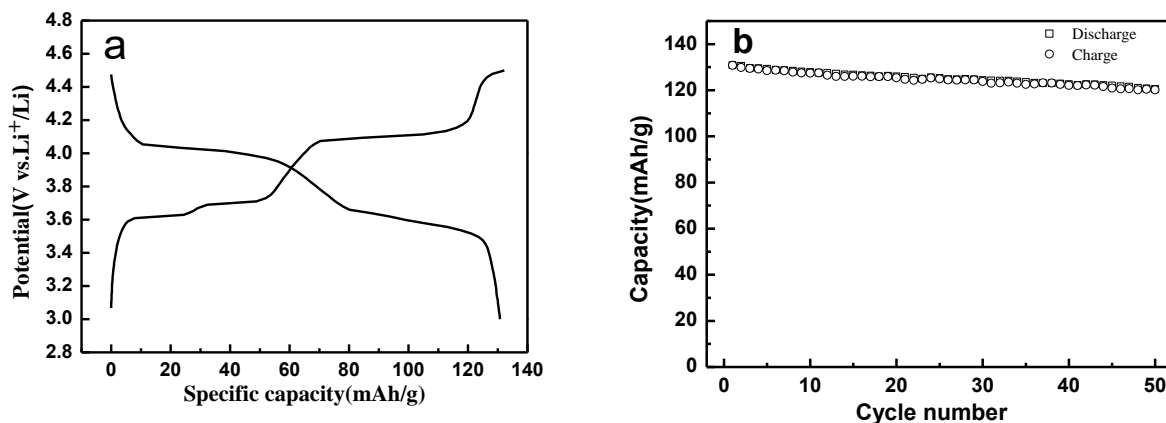
Figure 3 shows a representative TEM image of a sample annealed at 800 °C, with dark and light grey regions representing  $\text{Li}_3\text{V}_2(\text{PO}_4)_3$  and carbon, respectively. The above result confirmed the successful synthesis of carbon-coated  $\text{Li}_3\text{V}_2(\text{PO}_4)_3$ , with the presence of carbon being important due to inhibiting the growth of  $\text{Li}_3\text{V}_2(\text{PO}_4)_3$  grains, improving interparticle contact, and increasing the electrical conductivity of the composite[14]. Moreover, clear lattice fringes with a  $d$ -spacing of 0.36 nm were observed, corresponding to the (130) planes of monoclinic  $\text{Li}_3\text{V}_2(\text{PO}_4)_3$ .



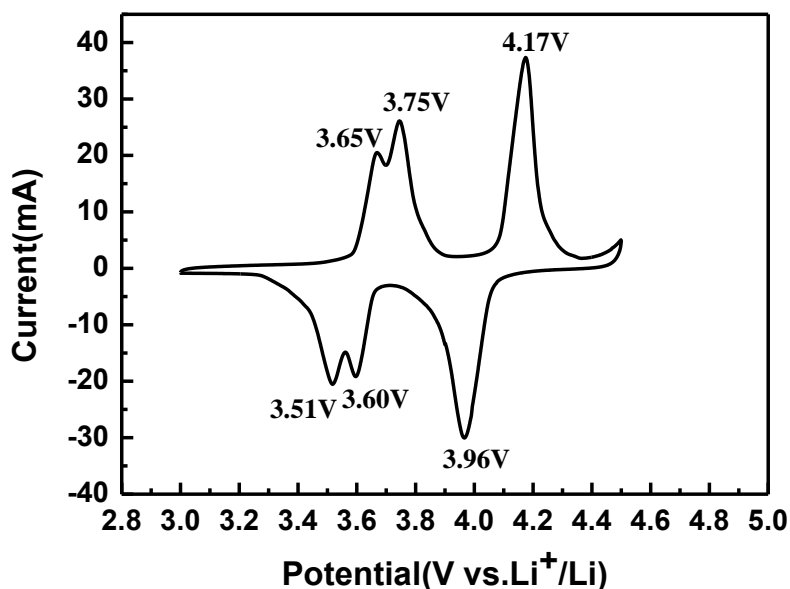
**Figure 3.** TEM images of  $\text{Li}_3\text{V}_2(\text{PO}_4)_3/\text{C}$ .

Figure 4 displays the first charge-discharge profiles and cycling curves of the prepared composite recorded in the range of 3.0–4.5V at 0.1 C, with the three plateaus observed at 3.59, 3.67, and 4.08V corresponding to  $\text{Li}_3\text{V}_2(\text{PO}_4)_3 \rightarrow \text{Li}_{2.5}\text{V}_2(\text{PO}_4)_3$ ,  $\text{Li}_{2.5}\text{V}_2(\text{PO}_4)_3 \rightarrow \text{Li}_2\text{V}_2(\text{PO}_4)_3$ , and  $\text{Li}_2\text{V}_2(\text{PO}_4)_3 \rightarrow \text{LiV}_2(\text{PO}_4)_3$  phase transitions, respectively[15]. The initial discharge capacity of LVP/C was determined as  $130.8 \text{ mAh}\cdot\text{g}^{-1}$ , being almost equal to the theoretical capacity of  $133 \text{ mAh}\cdot\text{g}^{-1}$ . The

capacity cycling curve of the synthesized composite indicated improved charge-discharge performance and cycling stability. Thus, after 50 cycles, a discharge capacity of  $120.2 \text{ mAh}\cdot\text{g}^{-1}$  was observed, corresponding to a capacity retention of 91.9%. Compared with literature : with  $125.5 \text{ mAh}\cdot\text{g}^{-1}$  for  $800^\circ\text{C}$ -prepared  $\text{Li}_3\text{V}_2(\text{PO}_4)_3$  composite [16], the excellent performance of charge and discharge is shown.



**Figure 4.** (a) The initial charge/discharge curves of  $\text{Li}_3\text{V}_2(\text{PO}_4)_3/\text{C}$  materials in the voltage range of 3.0-4.5V. (b) the cycle performances of  $\text{Li}_3\text{V}_2(\text{PO}_4)_3/\text{C}$  at 0.1C.



**Figure 5.** Cyclic voltammetry curves of  $\text{Li}_3\text{V}_2(\text{PO}_4)_3/\text{C}$  materials at a sweep rate of  $0.1 \text{ mV}^{-1}$  in the potential range of 3.0 to 4.5V

CV curves (Fig.5) of  $\text{Li}_3\text{V}_2(\text{PO}_4)_3/\text{C}$  contained three oxidation and three reduction peaks, in good agreement with the charge/discharge plateaus presented in Fig.4. The first two oxidation peaks around 3.65 and 3.75V were assigned to the two-step removal of the first Li, since there is an ordered

$\text{Li}_{2.5}\text{V}_2(\text{PO}_4)_3$  phase. However, the extraction of the second Li occurred in a one-step fashion at 4.17V, corresponding to the complete oxidation of  $\text{V}^{3+}$  to  $\text{V}^{4+}$ [17]. The three reduction peaks located at 3.96, 3.60, and 3.51V were attributed to the reinsertion of the two  $\text{Li}^+$  ions and the corresponding  $\text{V}^{4+}/\text{V}^{3+}$  redox processes[18-19].

The electrochemical impedance spectrum (Nyquist plot) presented in Fig. 6 contains two sections, namely a semicircle in the high-frequency range and a straight line with a slope of  $45^\circ$  in the low-frequency range[20], with the former representing charge transfer resistance and double-layer capacitance, and the latter representing the diffusion of  $\text{Li}^+$  in the solid phase and corresponding to Warburg impedance. The magnitude of the observed impedance is related to the charge transfer and lattice position of Li ions, being positively correlated to the semicircle radius and negatively correlated to the straight line slope. Specifically, the charge transfer impedance of samples prepared at  $800^\circ\text{C}$  equaled  $156\Omega$ , corresponding to good electrochemical performance.

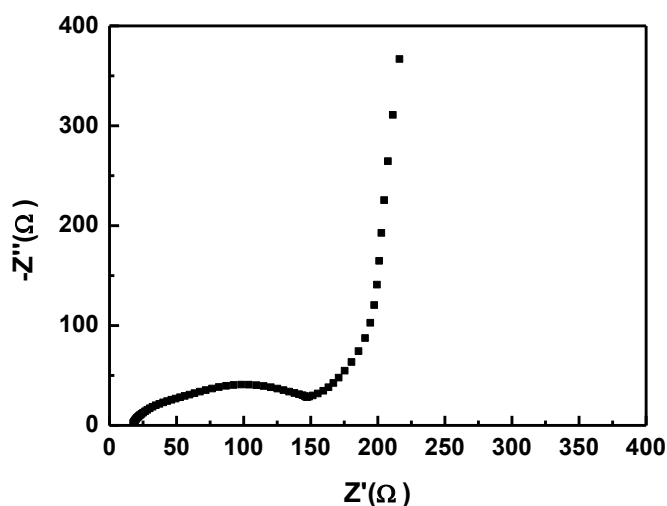


**Figure 6.** AC impedance spectra of  $\text{Li}_3\text{V}_2(\text{PO}_4)_3/\text{C}$  at  $800^\circ\text{C}$  for 12h.

#### 4. CONCLUSION

Herein, we describe the two-step synthesis of a monoclinic  $\text{Li}_3\text{V}_2(\text{PO}_4)_3/\text{C}$  composite, the unique three-dimensional architecture of which provides pathways for effective and rapid Li ion transfer. When calcination was performed at  $800^\circ\text{C}$  for 12h, the first-discharge specific capacity reached  $130.8 \text{ mAh}\cdot\text{g}^{-1}$  at 0.1 C in the range of 3–4.5 V, with capacity retention after 50 cycles being as high as 91.9%. Additionally, electrochemical impedance spectroscopy showed that the obtained composite had a small charge transfer resistance, confirming that  $\text{Li}_3\text{V}_2(\text{PO}_4)_3/\text{C}$  is a promising cathode material for Li-ion batteries and other energy storage devices.

#### ACKNOWLEDGMENTS

The study was supported by the National Natural Science Foundation of China (No. 21661030)

## References

1. X. Shi, W. Zhou, D. Ma, Q. Ma, D. Bridges, Y. Ma, *Journal of Nanomaterials*, 16 (2015) 122.
2. X. Wang, X. Cao, L. Bourgeois, H. Guan, S. Chen, Y. Zhong, *Adv. funct. mater.*, 22 (2012) 2682.
3. H. K. Song, K. T. Lee, G. K. Min, L. F. Nazar, J. Cho, *Advanced Functional Materials*, 20 (2010) 3818.
4. D. Sun, J. Li, J. Mai, Y. Fang, *Ceramics International*, 42 (2016) 7390.
5. C. L. Zhang, H.S. Li, N. Ping, G. Pang, G.Y. Xu, X.G. Zhang, *RSC Adv.*, 4 (2014) 38791.
6. S. Jing, X.L. Wu, J.S. Lee, J. Kim, Y.G. Guo, *J. Mater. Chem. A*, 1 (2013) 2508.
7. X.H. Rui, N. Ding, J. Liu, C. Li, C.H. Chen, *Electrochimica Acta*, 55 (2010) 2384.
8. X.H. Rui, C. Li, J. Liu, T. Cheng, C.H. Chen, *Electrochimica Acta*, 55 (2010) 6761.
9. H.W. Liu, C.X. Cheng, X.T. Huang, J.L. Li, *Electrochimica Acta*, 55 (2010) 8461.
10. Y.Q. Qiao, J.P. Tu, X.L. Wang, D. Zhang, J.Y. Xiang, Y.J. Mai, C.D. Gu, *Journal of Power Sources*, 196 (2011) 7715.
11. Y.Q. Qiao, J.P. Tu, J.Y. Xiang, X.L. Wang, Y.J. Mai, D. Zhang, W.L. Liu, *Electrochimica Acta*, 56 (2011) 4139.
12. W. Duan, Z. Hu, K. Zhang, F. Cheng, Z. Tao, J. Chen, *Nanoscale*, 5 (2013) 6485.
13. M.M. Ren, Z. Zhou, Y.Z. Li, X.P. Gao, J. Yan, *J. Power Sources*, 162 (2006) 1357.
14. H. Wang, Y. Li, C. Huang, *Journal of Power Sources*, 208 (2012) 282.
15. X. Nan, C. Zhang, C. Liu, M. Liu, Z. L. Wang, G. Cao, *ACS Applied Materials & Interfaces.*, 8 (2016) 862.
16. J. Yan, Y. Cao, F. Liu, *Rsc Advances*, 6 (2016).
17. L. Mai, S. Li, Y. Dong, Y. Zhao, Y. Luo, H. Xu, *Nanoscale*, 5 (2013) 4864.
18. X. J. Zhu, Y. X. Liu, L. M. Geng, L. B. Chen, *J. Power Sources*, 184 (2008) 578.
19. L. Wang, X. Zhou, and Y. Guo. *Journal of Power Sources*, 195 (2010) 2844.
20. B. Tian, J. Światowska, V. Maurice, S. Zanna, A. Seyeux, L. H. Klein, *Journal of Physical Chemistry C*, 117 (2015) 21651.

© 2018 The Authors. Published by ESG ([www.electrochemsci.org](http://www.electrochemsci.org)). This article is an open access article distributed under the terms and conditions of the Creative Commons Attribution license (<http://creativecommons.org/licenses/by/4.0/>).